

Article

Açaí (*Euterpe oleracea* Mart.) Seed Extracts from Different Varieties: A Source of Proanthocyanidins and Eco-Friendly Corrosion Inhibition Activity

Gabriel Rocha Martins ¹, Douglas Guedes ², Urbano Luiz Marques de Paula ¹, Maria do Socorro Padilha de Oliveira ³, Marcia Teresa Soares Lutterbach ⁴, Leila Yone Reznik ², Eliana Flávia Camporese Sérvulo ², Celuta Sales Alviano ⁵, Antonio Jorge Ribeiro da Silva ¹ and Daniela Sales Alviano ^{5,*}

¹ Instituto de Pesquisas de Produtos Naturais, Bloco H, Centro de Ciências da Saúde, Universidade Federal do Rio de Janeiro. Av. Carlos Chagas Filho, 373, Cidade Universitária, Rio de Janeiro 21941-902, Brazil; gabrielmartins@gmail.com (G.R.M.); urbanomarques@outlook.com (U.L.M.d.P.); ajorge@ippn.ufrj.br (A.J.R.d.S.)

² Escola de Química, Bloco E, Centro de Tecnologia, Universidade Federal do Rio de Janeiro. Av. Athos da Silveira Ramos, 149, Cidade Universitária, Rio de Janeiro 21941-909, Brazil; douglas.guedes.ferreira@gmail.com (D.G.); lreznik@eq.ufrj.br (L.Y.R.); eliana@eq.ufrj.br (E.F.C.S.)

³ Embrapa Amazônia Oriental–Trav. Dr. Enéas Pinheiro, s/n.–Belém, Pará 66095-100, Brazil; socorro-padilha.oliveira@embrapa.br

⁴ Instituto Nacional de Tecnologia, Divisão de Degradação e Corrosão. Av. Venezuela, 82, Rio de Janeiro 20081-312, Brazil; marcia.lutterbach@int.gov.br

⁵ Instituto de Microbiologia Paulo de Góes, Bloco I, Centro de Ciências da Saúde, Universidade Federal do Rio de Janeiro. Av. Carlos Chagas Filho, 373, Cidade Universitária, Rio de Janeiro 21941-902, Brazil; alviano@micro.ufrj.br

* Correspondence: danielalviano@micro.ufrj.br; Tel.: +55-21-3938-6711



Citation: Martins, G.R.; Guedes, D.; Marques de Paula, U.L.; de Oliveira, M.d.S.P.; Lutterbach, M.T.S.; Reznik, L.Y.; Sérvulo, E.F.C.; Alviano, C.S.; Ribeiro da Silva, A.J.; Alviano, D.S. Açaí (*Euterpe oleracea* Mart.) Seed Extracts from Different Varieties: A Source of Proanthocyanidins and Eco-Friendly Corrosion Inhibition Activity. *Molecules* **2021**, *26*, 3433. <https://doi.org/10.3390/molecules26113433>

Academic Editor: Maria Carla Marcotullio

Received: 30 April 2021
Accepted: 31 May 2021
Published: 5 June 2021

Publisher's Note: MDPI stays neutral with regard to jurisdictional claims in published maps and institutional affiliations.



Copyright: © 2021 by the authors. Licensee MDPI, Basel, Switzerland. This article is an open access article distributed under the terms and conditions of the Creative Commons Attribution (CC BY) license (<https://creativecommons.org/licenses/by/4.0/>).

Abstract: *Euterpe oleracea* Mart. (Arecaceae) is an endogenous palm tree from the Amazon region. Its seeds correspond to 85% of the fruit's weight, a primary solid residue generated from pulp production, the accumulation of which represents a potential source of pollution and environmental problems. As such, this work aimed to quantify and determine the phytochemical composition of *E. oleracea* Mart. seeds from purple, white, and BRS-Pará açaí varieties using established analytical methods and also to evaluate it as an eco-friendly corrosion inhibitor. The proanthocyanidin quantification (*n*-butanol/hydrochloric acid assay) between varieties was 6.4–22.4 (*w/w*)/dry matter. Extract characterization showed that all varieties are composed of B-type procyanidin with a high mean degree of polymerization ($mDP \geq 10$) by different analytical methodologies to ensure the results. The purple açaí extract, which presented 22.4% (*w/w*) proanthocyanidins/dry matter, was tested against corrosion of carbon steel AISI 1020 in neutral pH. The crude extract (1.0 g/L) was effective in controlling corrosion on the metal surface for 24 h. Our results demonstrated that the extracts rich in polymeric procyanidins obtained from industrial açaí waste could be used to inhibit carbon steel AISI 1020 in neutral pH as an abundant, inexpensive, and green source of corrosion inhibitor.

Keywords: proanthocyanidins; degree of polymerization; green corrosion inhibitor; white açaí; BRS-Pará; phenolic compounds; residue exploitation; mass spectrometry analysis; açaí seeds

1. Introduction

Euterpe oleracea Mart., an endogenous palm tree of the Amazonian biome that grows in flooded areas, produces a dark purple fruit called açaí [1]. Its edible pulp is rich in antioxidants and nutrients to the most impoverished local populations [2] and now commercialized as a functional food [3]. Açaí has high nutritional value due to the predominance of fatty acids and amino acids. However, the antioxidant capacities of high contents of

anthocyanins (cyanidin 3-glucoside and cyanidin 3-rutinoside) and other flavonoids are associated with açai's health benefits against several diseases related to oxidative stress [4].

Traditionally, açai is a purple globose fruit. However, it can be found in a green to yellow color with a crême mesocarp, commonly referred to as “white açai” [3,5]. Additionally, Embrapa Eastern Amazonia (Belém, Pará, Brazil) has developed a cultivar, the BRS-Pará, suitable for growing on stable land, making the production more high-yielding than the traditional system [6].

When fully ripe, the açai fruit has a deep purple peel (epicarp), a small fleshy pulp (pericarp), and a single seed covered by a thin mesocarpic fiber (endocarp). Only 15% (*w/w*) of açai is edible, generating seeds as the primary agricultural residue from depulping [2,7–9]. A small part is used in jewelry craft, food for pigs, decomposed into potting soil for home gardens, or burned for fuel, but most of it is just thrown away after pulp production [3].

An increasing number of publications has reported that polyphenols such as catechin, epicatechin, and oligomeric proanthocyanidins (PACs) are extractable from açai seeds [10–12]. Reports with medicinal applications for the açai seed extracts also showed protective effects against emphysema, lung inflammation, oxidative stress, cardiovascular dysfunction, and many other biological activities [13–15]. Most of them correlated PACs in açai seed extracts with the observed pharmacological effects.

PACs are widespread in the Plant Kingdom, being the second largest group of polyphenols after lignins. They are composed of polyphenolic oligomers or polymers consisting of units of flavan-3-ol linked mainly through C4 to C8 or C4 to C6 interflavan bonds (B-type), and even an additional ether bond O7 to C2 or O5 to C2 (A-type) [16].

Despite its pharmacological properties, the bioavailability of PACs is primarily influenced by their degree of polymerization (DP). Oligomers with $DP \geq 4$ do not pass the gut barrier, thus having limited applicability as pharmaceuticals [17]. However, high-weighted oligomers have been explored as an abundant, inexpensive, green source for adhesives, coatings, and resin productions for the industry [18–20], which prevents their accumulation in nature [21].

Corrosion is a material deterioration caused by chemical, electrochemical, and biological reactions. The global cost of corrosion is estimated at USD 2.5 trillion [22]. Effective prevention practices could result in substantial savings of 15–35% of the annual corrosion cost damage [22]. Natural products have been widely tested for metal protection from corrosion. The exploitation of agro-industrial residues' anticorrosive potential has risen as an eco-friendly alternative, especially when considering the high availability, low cost, and potential for anticorrosive compounds of biomass wastes that garner less environmental concern and have fewer harmful effects than synthetic anticorrosives [23]. PAC extracts inhibit corrosion in several ways: as metal surface treatment agents, as oxygen scavengers, or as films (coating and cathodic film former) [24]. Mangrove (*Rhizophora* spp.) and coconut (*Cocos nucifera* L.) extracts enriched with these compounds, for example, have shown corrosion inhibition properties in different pH solutions [25–27].

A crucial step towards the agreement with global priorities and assessments of the United Nations (UN) 2030 Sustainable Development Agenda is using renewable raw materials in the sustainable production of by-products [28]. In this respect, Brazil has excellent potential to exploit agro-industrial residues, such as açai seeds. Preliminary studies showed that PACs are a large part of the seed's composition. This fact led us to the investigation of whether seed extracts of different açai varieties (purple, white, and BRS-Pará) would possibly work as a source of bioactive PACs, which could be exploited in pharmaceuticals, food, and cosmetic applications. Furthermore, the determination of their anticorrosive properties could be a cheap, abundant, and green corrosion inhibitor, adding value for this by-product of the açai industry.

2. Results and Discussion

The potential health benefits attributed to açai seed extracts [29–31] highlight how critical comprehensive chemical characterization is. Research on the seed extract's new biological effects is associated with its composition, thus adding value to this residue. Therefore, we started to investigate the chemical composition of varieties of açai seeds: purple açai (PA), white açai (WA), and BRS-Pará (BRS).

The results from the extraction and liquid–liquid partitioning yields are shown in Table 1. The extraction generated 6.99% (*w/w*), 7.61% (*w/w*), and 8.04% (*w/w*) yields for BRS, WA, and PA, respectively. Liquid–liquid partitioning with ethyl acetate and water 1:1 (*v/v*) can separate PACs by size since only small weighted ones and other polyphenols are soluble in ethyl acetate. The aqueous fractions yielded above 75%, indicating that all varieties exhibited a high number of polymeric PACs.

Table 1. Extraction, liquid–liquid partition, mDP, and n-BuOH/HCl result from PA, WA, and BRS samples.

Results/Samples	PA	WA	BRS
Extraction yield (%)	8.04 (±0.85)	7.61 (±0.78)	6.99 (±1.25)
Liquid–Liquid Partitioning			
EtOAc fraction yield (%)	9.6	15.6	8.7
Aqueous fraction yield (%)	87.4	83.1	75.9
PAC content (%/dry matter)	22.4 ± 5.0	6.4 ± 0.6	11.5 ± 3.8
mDP by acid catalysis	10.29 ± 0.01 [0.07]	11.23 ± 0.09 [0.84]	11.81 ± 0.09 [0.74]
Terminal subunit composition in (%) of (+)-catechin	86.22 ± 0.19 [0.22]	83.28 ± 0.34 [0.41]	84.91 ± 0.51 [0.61]
Conversion yield (%)	98.7	84.3	121.5

PA—purple açai, WA—white açai, BRS—BRS-Pará açai cultivar, EtOAc—ethyl acetate, mDP—mean degree of polymerization.

After extraction, the content of PACs was quantified by n-butanol/hydrochloric acid assay following a published protocol [32]. PA exhibited 22.4% (*w/w*) proanthocyanidins/dry matter, while WA displayed 6.4% (*w/w*) and BRS 11.5% (*w/w*). Thus, these results show that açai seed can be exploited as a source of polymeric proanthocyanidins.

The crude extracts were also analyzed using hydrophilic interaction chromatography (HILIC). A diol column separates PACs by size, allowing the report of results to be given in degree of polymerization (DP) after calibration [33]. A fluorescence detector (FLD) and mass spectrometry detector (micro-TOF) were used for comparison. Commercially available standards of epicatechin and procyanidin B2 were injected for retention time calibration for both methods (data not shown). Using the HILIC–HPLC–FLD analysis (Supplementary Material, Figure S1), PA, WA, and BRS crude extracts displayed individual peaks representing a degree of polymerization from 1 up to 12. The asymmetry in the peaks could indicate different PAC types in the samples or low column resolution [34].

The extracted ion chromatograms (EIC) from the HPLC–DAD–ESI–TOF–MS analysis (Supplementary Material, Figure S2–S4) were obtained using the molecular formula for procyanidins. The retention time showed peaks eluting in the increasing order of DP. PA and BRS crude extracts exhibited *m/z* 289, 577, 865 and 1153 ($\Delta = 288$) of $[M-H]^-$ characteristic of (epi)catechin and B-type, dimer, trimer, and tetramer, respectively. The *m/z* 720, 864, and 1008 ($\Delta = 144$) represented the $[M-2H]^{2-}$ of B-type procyanidin pentamer, hexamer, and heptamer. The *m/z* ion of 575 was indicative of $[M-4H]^{4-}$ B-type procyanidin octamer. WA crude extract exhibited the same profile except for a B-type procyanidin octamer signal.

The results obtained from HILIC–HPLC–FLD and HILIC–HPLC–DAD–ESI–TOF–MS are comparable. However, it also displays how the disparity between the results can arise, for instance, from analytical differences. Both methodologies showed that açai seeds (*E. oleracea* Mart.) crude extracts are composed of oligomeric procyanidins, even though HILIC–HPLC–FLD indicated a higher degree of polymerization in the extracts.

The ethyl acetate fractions were analyzed by direct infusion ESI-MS/MS in negative mode (Table 2). PA and BRS displayed an m/z 289.2 ion, with MS² fragments with m/z 245 (a CO₂ loss) and m/z 205 (C₄H₄O₂ loss from the A-ring) ions indicative of (epi)catechin. An m/z 421.3 (289 + 132 Da) ion characteristic of a (epi)catechin-pentoside with a fragment of m/z 289.34 was found. Both samples exhibited an m/z 577.2 ion with MS² fragments of m/z 425 and m/z 407 (425-H₂O) characteristic of a retro-Diels–Alder (RDA) fission of B-type procyanidin dimer. It also displayed a MS² fragment of m/z 451, a product of heterocyclic ring fission (HRF), and MS² fragments of m/z 287 and m/z 289, indicative of a quinone methide fission [35].

Table 2. PA, WA, and BRS EtOAc fractions by ESI-MS/MS direct infusion.

PA		WA		BRS		Identification
Molecular ion [M – H] [–] (m/z)	MS ² (m/z)	Molecular ion [M – H] [–] (m/z)	MS ² (m/z)	Molecular ion [M – H] [–] (m/z)	MS ² (m/z)	
289.1	245; 205	289.1	245; 205	289.1	245; 205	(epi)catechin
577.2	425; 407; 289; 451; 287	577.2	407; 425; 289; 451; 287	577.2	451; 425; 407; 289; 287	B-type procyanidin dimer
421.28	289	421.2	289	421.25	289	(epi)catechin- pentoside
-	-	469.1	289	-	-	Unknown compound

PA—purple açai, WA—white açai, BRS—BRS-Pará açai cultivar.

The WA EtOAc fraction exhibited the same ions and fragmentation pattern of PA and BRS varieties, except for an unidentified compound with m/z 469 ion and an MS² of m/z 289. This confirms that procyanidins are the main polyphenols in the açai seeds, as corroborated by the literature [10–12,36].

As established by the liquid–liquid partitioning, the aqueous fractions are rich in polymeric PACs. Therefore, it was used for phloroglucinolysis of all varieties, and the results are shown in Table 1 (chromatograms are available in Supplementary Material, Figure S5). All varieties exhibited similar results, with a subunit composition profile of (–)-epicatechin as the single extension subunit found and a high percentage for (+)-catechin as a terminal subunit (above 80%). Their mean degree of polymerization (mDP) was also comparable, PA exhibited an mDP of 10.29, WA had an mDP of 11.23, while BRS aqueous fraction displayed an mDP of 11.81. Conversion yields for all the samples were above 80% which favors the homogeneity of the results. All açai varieties presented a high polymerized B-type procyanidin. A previous study indicated similar results for açai seed extracts with a high (–)-epicatechin content for extension subunit (above 95%), a high (+)-catechin percentage as terminal subunit (above 60%), and an mDP between 9.7–13 [11], corroborating that açai seed extract might be a source of bioactive procyanidins, adding value to this by-product while decreasing the environmental impact.

MALDI-TOF mass spectra of PA, WA, and BRS aqueous fractions (Supplementary Material, Figure S6) showed clear repetitive patterns of peaks that allow the identification of specific oligomer series. Table 3 shows the possible combinations of different repeating units and the corresponding degrees of polymerization. All peaks correspond to sodium ion adducts (+23 Da) in the positive ion mode. The PA aqueous fraction had peak ions, indicating the presence of a B-type procyanidin series of DP = 3 up to 11 (889.7, 1177.8, 1466.1, 1754.5, 2042.6, 2330.8, 2619.0, 2907.0, 3195.4) because of repeating units (Δ = +288 Da) characteristic to procyanidin units. Results also show a heterogeneous series with one prodelphinidin unit substitution (904.8, 1193.3, 1481.5, 1770.0, 2058.0, 2346.0, 2634.3, 2921.9, 3211.0) with DP = 3 to 11 and B-type linkages. A variation of m/z +16 units is indicative of the presence of a hydroxyl group. Furthermore, a B-type procyanidin series with one galloyl substitution was identified (1329.4, 1618.6, 1906.5, 2193.4, 2483.5, 2771.0, 3058.1) with DP = 4 up to 10 (galloyl esterification displays a Δ = +152 Da). The BRS aqueous fraction also had the same pattern with a B-type procyanidin series (DP = 3–11), a

procyanidin–prodelphinidin heterogeneous series (DP = 3–11), and a B-type procyanidin with one galloyl substitution (DP = 4–10). WA showed similar patterns with a B-type procyanidin (with DP = 3–11) and heterogeneous procyanidin–prodelphinidin sequences (with DP = 3–10). However, it did not have a galloyl substitution sequence.

Table 3. PA, WA, and BRS aqueous fractions MALDI-TOF [M+Na]⁺ mass spectra.

DP	PA		WA		BRS		
	Predicted [M + Na] ⁺ (Da)	Observed [M + Na] ⁺ (Da)	Observed [M + Na] ⁺ (Da)	Observed [M + Na] ⁺ (Da)	Monomeric Units		
					(epi)catechin	(epi)gallocatechin	Galloyl
3	889.8	889.7	889.9	889.6	3	0	0
	905.8	904.8	905.8	905.5	2	1	0
4	1178.0	1177.8	1178.2	1177.9	4	0	0
	1194.0	1193.3	1194.2	1193.8	3	1	0
	1330.1	1329.4	-	1330.0	4	0	1
5	1466.3	1466.1	1466.6	1466.2	5	0	0
	1482.3	1481.5	1482.8	1482.0	4	1	0
	1618.4	1618.6	-	1618.3	5	0	1
6	1754.5	1754.5	1755.7	1754.4	6	0	0
	1770.5	1770.0	1771.3	1770.1	5	1	0
	1906.6	1906.5	-	1906.4	6	0	1
7	2042.8	2042.6	2043.9	2042.7	7	0	0
	2058.8	2058.0	2060.1	2058.6	6	1	0
	2194.9	2193.4	-	2194.4	7	0	1
8	2331.0	2330.8	2332.6	2330.9	8	0	0
	2347.0	2346.0	2347.8	2346.3	7	1	0
	2483.1	2483.5	-	2483.5	8	0	1
9	2619.3	2619.0	2621.3	2619.1	9	0	0
	2635.3	2634.3	2636.4	2634.4	8	1	0
	2771.4	2771.0	-	2770.9	9	0	1
10	2907.6	2907.0	2907.5	2907.1	10	0	0
	2923.5	2921.9	2924.6	2922.6	9	1	0
	3059.6	3058.1	-	3059.7	10	0	1
11	3195.8	3195.4	3196.2	3195.1	11	0	0
	3211.8	3211.0	-	3210.6	10	1	0

Heterogeneous sequences with procyanidin–prodelphinidin units in other plants are commonly reported in the literature [27,37]. All açai varieties exhibited an arrangement with a one-unit exchange from procyanidin for prodelphinidin. Nevertheless, the phloroglucinolysis reaction and MALDI-TOF data were consistent, showing that B-type procyanidins are the major components in the aqueous fractions of *Euterpe* spp. analyzed.

The *E. oleracea* Mart. seeds (PA, WA, and BRS varieties) are by-products with no primary exploration and with ecological implications due to accumulation. PA seed extract displayed a higher concentration of PACs (BuOH/HCl assay) and, therefore, was chosen for the corrosion experiments.

The PA crude extract corrosion inhibition activity was analyzed after 24 h of immersion in corrosive solution by fitting an LPR curve with ANOVA software to calculate the Tafel parameters, shown in Table 4, and by potentiodynamic curves (Figure 1). The PA crude extract only promoted an expressive effect at the concentration of 1.0 g/L, both increasing the corrosion potential (E_{corr}) and polarization resistance. The effect on E_{corr} suggests an anodic type of corrosion inhibitor, but the increasing polarization resistance is typical for the cathodic type of corrosion inhibitor. Therefore, PA crude extract behavior suggests inhibition for both cathodic and anodic reactions [38,39].

The PA crude extract efficiency as a corrosion inhibitor was estimated by corrosion current density (J_{corr}) and by polarization resistance (R_p) of the metallic surface to evaluate the metal susceptibility to corrosion and the stability of the protective film on the metal surface, respectively. Table 4 shows that the anticorrosion activity occurred only at the concentration of 1.0 of PA crude extract. This data was corroborated by corrosion rate, also shown in Table 4. The efficiency of a corrosion inhibitor depends on a concentration range with an ideal number of molecules to form a stable, protective film. The absence or abundance of molecules leads to unstable film formation, either due to an insufficient number of molecules or the dispute of metallic surface interaction by excess of molecules [39].

Table 4. Galvanostatic and linear polarization resistance (LPR) parameters for AISI 1020 carbon steel in neutral pH with various PA concentrations after 24 h of immersion.

Concentration (g/L)	Tafel Data					LPR Data		Corrosion Rate (mm/year)
	E_{corr} (mV, SCE)	β_{anodic} (mVdec ⁻¹)	β_{cathodic} (mVdec ⁻¹)	J_{corr} (mAcm ⁻²)	η_{Tafel}	R_p (Ωcm^2)	η_{LPR}	
0	−732	0.03819	0.03836	6.215×10^{-6}	-	1.22×10^3	-	0.072216
0.1	−696	0.05404	0.14260	2.465×10^{-5}	0	633.6	0	0.28638
0.2	−701	0.06467	0.02803	2.298×10^{-5}	0	724.9	0	0.26704
0.5	−698	0.03672	0.10310	1.254×10^{-5}	0	710.6	0	0.14569
0.8	−700	0.04628	1.74730	2.334×10^{-5}	0	749	0	0.27126
1.0	−556	0.00655	0.00592	5.122×10^{-10}	99.99	1.75×10^6	99.93	5.92×10^{-6}

E_{corr} —corrosion potential; J_{corr} —corrosion current density; η_{Tafel} —inhibition efficiency calculated with J_{corr} values and zero standardized for negative values; R_p —polarization resistance; η_{LPR} —inhibition efficiency calculated with R_p values.

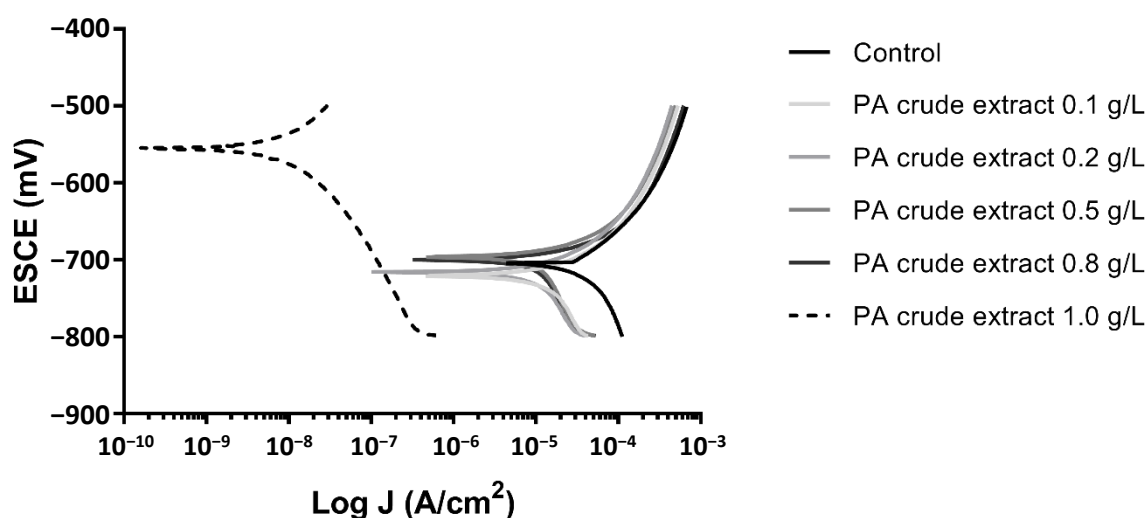


Figure 1. Potentiodynamic curves of carbon steel AISI 1020 after 24 h in neutral pH corrosive solution for different concentrations of PA crude extract.

The corrosion inhibitor efficiency of over 99.9% and a considerable reduction of corrosion rate shows that 1.0 g/L of PA crude extract, in neutral pH after 24 h of immersion, is a promising green corrosion inhibitor. Furthermore, the efficiency obtained for 1.0 g·L⁻¹ of PA crude extract is higher than studies with PACs from other natural sources [25,26].

The Tafel slopes of 0.1 to 0.8 g/L and corrosion rate data showed a more intense corrosive process than that observed for the control (absence of inhibitor). These results prove that a weak corrosion inhibitor can promote the corrosive process [39,40]. However, the significant reduction on the anodic (β_{anodic}) and cathodic (β_{cathodic}) coefficients in the presence of 1.0 g/L¹ of PA crude extract shows the importance of the ideal concentration of inhibitor for inhibition of corrosion reactions.

The potentiodynamic curves (Figure 1) corroborated the suggestion that PA crude extracts affect anodic and cathodic reactions. After 24 h of immersion, in the condition of 1.0 g/L of PA crude extract, both anodic and cathodic branches showed low values of current density compared to the control. The other tested concentrations showed similar curves to those observed for the control.

Adsorption inhibitors affect the corrosion reaction in anodic and cathodic branches, as observed in the presence of 1.0 g/L of PA crude extract with a significant reduction of corrosion current density (Figure 1). This behavior is standard in organic compounds, such as PACs, for which there are already records in the literature [25–27,41]. The protective film was formed by adsorption of molecules on the metal surface, as the black/dark purple film on the metal surface in 1.0 g/L of PA crude extract was observed (Supplementary, Figure S7).

The effect of PACs on the metal surface was analyzed through EIS, displayed as Nyquist and Bode plots (Supplementary Material, Figures S8 and S9). The impedance consists of the relation between the alternating potential and the alternating current in the response of known frequency applications. Although the impedance is inversely proportional to the current, higher impedance modules promote lesser corrosion susceptibility. For the Nyquist plot in the presence of PA 1.0 g/L crude extract, the semicircle suggests the formation of a protective layer, blocking or reducing the effect of corroding molecules of the electrolyte on the metal surface. In the Bode plot with PA 1.0 g/L crude extract, there is a peak of the phase angles at low frequency, corroborating the protective film formation on the metallic surface hypothesis. Thus, as observed in the Nyquist plot, the presence of PACs inhibits the corrosion process. Furthermore, lower concentrations (0.2–0.8 g/L) probably do not have a sufficient number of molecules to form an efficient protective layer. However, in 1.0 g/L, the molecules content is ideal for metal surface adsorption, avoiding corrosive processes.

Previous studies have revealed açai seeds as a promising source of antioxidants, with a higher antioxidant activity than the pulp bioactive compounds [7,11,12]. However, this is the first time that açai seed extracts were tested for corrosion inhibition activity. In the PA crude extract, the high radical scavenging capacity and reducing metal activity of PACs translated to a promising green corrosion inhibitor for carbon steel AISI 1020 in neutral pH conditions at room temperature.

The protective activity can be affected by inhibitor chemical composition, metal type, and experimental physicochemical conditions. These variables can affect (positively or negatively) the interaction between the inhibitor and the metallic surface and consequently its anticorrosion activity [42–44]. Especially for PACs, their origin affects the polymerization degree, and it involves the interaction with the metal surface and the stability of the protective film. It was previously described that polymeric PACs are more effective for metal surface protection than monomeric ones [27,42–44].

Crude extracts from açai (*E. oleracea* Mart.) seeds and coconut (*Cocos nucifera* L.) husk fiber are natural sources of phenolic compounds. Comparing the polymeric degree of PACs from these natural sources showed that those PACs from açai seed crude extracts had a higher polymeric degree than those from coconut husk fiber [25]. Furthermore, the PA crude extract proved to be more effective (higher inhibition efficiency and lower concentration) for carbon steel metal protection than coconut husk fiber crude extract. This supports the relation between high polymerization degree and corrosion inhibition activity.

3. Materials and Methods

3.1. Materials

Analytical grade acetone and HPLC grade methanol, acetonitrile, ethyl acetate, acetic acid, and formic acid used were obtained from TEDIA (Rio de Janeiro, Brazil). Water was purified using a Milli-Q system from Millipore (Billerica, MA, USA). Phloroglucinol, (+)-catechin, (–)-epicatechin, and procyanidin B2 (dimer) were purchased from Sigma-

Aldrich (St. Louis, MO, USA), and NaHCO_3 was acquired from Spectrum (New Brunswick, NJ, USA).

3.2. Extraction Procedures

E. oleracea Mart. seeds from purple açai (PA) and white açai (WA) were obtained in São João de Pirabas (Pará, Brazil) by a local private producer. The *E. oleracea* Mart. BRS-Pará (BRS) seeds were graciously donated by Embrapa Oriental Amazonia (Belém, Pará). The seeds had their pulps removed and were washed, air-dried, and transported to the laboratory. The seeds were grounded, defatted (20.0 g, triplicate) by Soxhlet extraction with *n*-hexane (3×4 h). The defatted powdered seeds were extracted (2.0 g, triplicate) with $\text{Me}_2\text{CO}:\text{H}_2\text{O}$ 6:4 in an ultrasound bath for three 10 min cycles, renewing solvent in each period. The crude extracts were vacuum filtered; the acetone was evaporated at 35°C in a rotatory evaporator and then lyophilized.

3.3. Ethyl Acetate:Water Liquid–Liquid Partitioning

Crude extracts were dissolved in 50 mL of water and then partitioned with the same volume of ethyl acetate three times. The organic phase was evaporated in a rotatory evaporator, and the aqueous fraction was lyophilized.

3.4. Proanthocyanidin Content by *n*-BuOH/HCl Test

The determination of proanthocyanidin content followed a published protocol [30]. The grounded and defatted seeds (0.2 g in triplicate) were submitted to ultrasound-assisted extraction with acetone:water 7:3 (10 mL) for 10 min. A 5 μL aliquot of extract was added to a sealed test tube containing 3 mL of *n*-butanol/hydrochloric acid (95:5) and 100 μL of a 2% solution of $\text{NH}_4\text{Fe}(\text{SO}_4)_2$ in 2N hydrochloric acid. The solution was heated for 60 min (95°C). After cooling, the absorbance was measured at 550 nm (UV-1601 Shimadzu spectrophotometer). Results were expressed in percentage (%) by dry matter.

3.5. HILIC–HPLC–FLD Proanthocyanidin Analysis

The HPLC (Perkin-Elmer Flexar) was equipped with a LC column oven, LC autosampler, quaternary LC pump, solvent manager, PDA, FLD detectors, and Chromera-Flexar software. A previously published protocol was followed [31], where samples were prepared by dissolving 1.0 mg of crude extract in acetonitrile/water 1:1 to 1.0 mg/mL and filtering through 0.22 μm PTFE filters. Aliquots of 10 μL were injected in a Merck LiChrospher[®] 100 diol column (250 \times 4.6 mm, 5 μm) with a LiChroCART guard column of the same material. The flow rate was 0.8 mL/min; the column temperature was 30°C , the fluorescence detector was set with excitation at 276 nm and emission at 316 nm. A binary mobile phase was used, namely acetonitrile:acetic acid (98:2) as phase A, and methanol:water:acetic acid (95:3:2) as phase B. Gradient elution: 0–35 min, 0–40% B, 35–40 min, 40% B, 40–45 min, 40–0% B. The column was washed for 10 min with 90% B followed by 20 min as re-equilibration time.

3.6. MALDI-TOF-MS

The mass spectrometry analyses were made on a MALDI-TOF Autoflex Speed Bruker spectrometer using a published protocol [35] with slight modifications. Samples (2 mg) were dissolved with 0.1% aqueous trifluoroacetic acid and diluted to 1:10 with DHB matrix solution (0.1% TFA). A 1.0 μL aliquot of aqueous sodium chloride (1.0 mg/mL) was added to the solution. The samples were applied to the MALDI plate (duplicate) and analyzed after they were dried. Analyses were made in positive mode, using a peptide calibration standard (Bruker, Billerica, MA, USA). Data were processed using mMass 5.5.0 software (Strohalm M.[®]).

3.7. Direct Infusion ESI-MS/MS Analysis

Ethyl acetate fractions were analyzed by direct infusion in an Amazon SL ESI-iontrap spectrometer (Bruker). Samples (1.0 mg) were diluted 1:100 with methanol and analyzed in negative mode. Infusion flow rate: 3 $\mu\text{L}/\text{min}$, nebulizer pressure: 10 psi, N_2 : 5 L/min, source temperature: 200 $^\circ\text{C}$.

3.8. Phloroglucinolysis

Phloroglucinolysis determinations used a previously published protocol [45] with a phloroglucinol solution prepared with 5.0 g of phloroglucinol, 1.0 g of ascorbic acid, and 0.1 N HCl in a minimum amount of methanol up to 100 mL. NaHCO_3 solution was prepared with 336.0 mg of NaHCO_3 and Milli-Q water up to 100 mL (40 mM).

Capped glass test tubes containing 5.0 mg weighted samples (triplicate) with 1.0 mL of the phloroglucinol solution were heated for 20 min in a water bath (50 $^\circ\text{C}$). An aliquot of 200 μL was transferred to a 2.0 mL vial, and 1.0 mL of the NaHCO_3 solution was added. A ReproSil-Pur RP-18 column (250 \times 4.6 mm, 5 μm , Dr. Maisch GmbH, Germany) with a guard column of the same material was used; flow rate: 1 mL/min, 280 nm UV detector. Mobile phase (A) was aqueous 1% acetic acid, and (B) was methanol. Gradient mode: 5% B for 10 min, 5–20% B in 20 min, 20–40% B in 25 min, 90% B for 10 min, 5% B for 5 min.

3.9. HPLC–DAD–ESI-TOF-MS

Analysis followed a protocol [46] with modifications. The HPLC–DAD analysis occurred using LiChrospher[®] 100 diol (250 \times 4.6 mm, 5 μm , Merck) with guard column LiChroCART of the same material at 30 $^\circ\text{C}$. Two solvents were used: water with 1% (*v/v*) formic acid (A), and acetonitrile (B). The elution profile was 0–40 min, 95–35% (*v/v*) B in A (linear gradient); 40–45 min, 35–95% B in A (linear gradient); and 45–75 min 95% B in A (isocratic). The flow rate was 0.3 mL/min; $\lambda = 280$ nm. Injection volume was 10 μL (1 mg/mL). ESI-TOF-MS was in a Bruker's MicrOTOF II in negative mode, scan from *m/z* 100 to 1500, capillary set at 3000 V, offset endplate at -500 V, nebulizer at 4.0 bar, dry heater at 200 $^\circ\text{C}$, and dry gas at 10.0 L/min. Extracted ion chromatograms (EIC) were obtained using the molecular formula for procyanidins with ± 0.01 accuracy and intensity from 10^5 to 1000.

3.10. Corrosion Experiments

The corrosion tests were carried out in a three-electrode (a working electrode, a reference KCl-saturated calomel electrode (SCE), and a platinum counter electrode) electrochemical cell which was connected to an AUTOLAB PGSTAT302N potentiostat/galvanostat. Square coupons of carbon steel AISI 1020 (Fe–98.5%, C–0.2%, Mn–0.6% and traces of P, S, Si, Sn, Cu, Ni, Cr, and Mo) were used as working electrodes. The corrosive solution simulates cooling systems water and was composed of 500 ppm chloride (829 mg/L NaCl), 150 ppm of sulfate (222 mg/L Na_2SO_4), and 150 ppm of calcium carbonate (CaCO_3). The pH electrolyte was controlled in neutral range (7.0 ± 0.2) during all immersion times with different concentrations of PA crude extract (0–1.0 g/L).

These tests were conducted in 800 mL glass cells, maintained at controlled temperature (25 ± 2 $^\circ\text{C}$), and slow shaken for 24 h for data acquisition. Before each test, carbon steel AISI 1020 coupons (working electrodes), with 1.0 cm^2 of the exposed area, were mechanically polished using SiC papers of 80, 120, 220, 320, 400, 500 and 600 grit, washed with distilled water, cleaned with ethanol and dried in hot air. And, the lyophilized PA crude extract was resuspended in distilled water and sterilized by membrane filtration (0.22 mm pore) to prepare a stock solution, used as basis for the tests PA crude extract solutions.

The activity as corrosion inhibitor was determined through the comparison between the results in absence and presence of different concentrations of PACs in PA crude extract and performed using LPR and potentiodynamic curves techniques. The concentrations tested were 0.1, 0.2, 0.5, 0.8 and 1.0 g/L. The potentiodynamic polarization curves were performed by working electrode scanning from -800 to -500 mV/SCE at a scan rate of

0.33 mVs⁻¹. And the Tafel data acquisition applied linear polarization resistance (LPR) technique by working electrode scanning from -20 to 20 mVSCE around the corrosion potential at a scan rate of 0.33 mVs⁻¹. The inhibition efficiencies were calculated through two data. The first method applied Tafel data (Equation (1)), where J_{corr} and J_{corr}^0 are the corrosion current density values with and without inhibitor, respectively. The second one by linear polarization resistance (LPR) data (Equation (2)), where R_p and R_p^0 are the resistance polarisation values in the presence and absence of inhibitor.

$$\eta_{Tafel}(\%) = \frac{J_{corr}^0 - J_{corr}}{J_{corr}^0} \times 100 \quad (1)$$

$$\eta_{LPR}(\%) = \frac{R_p - R_p^0}{R_p} \times 100 \quad (2)$$

4. Conclusions

In this study, all analytical techniques determined that the three açai varieties (PA, WA and BRS-Pará) are a potential source of PACs with a high degree of polymerization, which could have industrial applications. All varieties exhibited a similar chemical composition, indicating that the seeds do not need to be separated to exploit their phenolics. Furthermore, PA crude extract showed itself as a promising green corrosion inhibitor for carbon steel AISI 1020 in neutral pH corrosive solutions at room temperature. A black/dark purple film was observed on carbon steel AISI 1020 surface after 24 h of immersion in the presence of 1.0 g/L of PA crude extract, suggesting the inhibitor adsorption and a protective film formation. The inhibition efficiency of over 99.9% indicated the açai seed extract is a promising target for future studies about corrosion inhibitors from natural sources, especially from a raw solid waste as the açai seeds.

Supplementary Materials: Figure S1—HILIC–HPLC–FLD chromatograms of PA, WA and BRS crude extracts. Peaks are identified by their degree of polymerization (DP). Figure S2—HPLC–DAD chromatogram of PA extract. Extracted ion chromatograms corresponding to B-type procyanidins oligomers (monomer, dimer, trimer, tetramer, pentamer, hexamer, heptamer and octamer, respectively). Figure S3—HPLC–DAD chromatogram of WA extract. Extracted ion chromatograms corresponding to B-type procyanidins oligomers (monomer, dimer, trimer, tetramer, pentamer, hexamer, heptamer and octamer, respectively). Figure S4—HPLC–DAD chromatogram of BRS extract. Extracted ion chromatograms corresponding to B-type procyanidins oligomers (monomer, dimer, trimer, tetramer, pentamer, hexamer, heptamer and octamer, respectively). Figure S5—Chromatograms of PA, WA and BRS phloroglucinolysis aqueous fractions. Figure S6—MALDI-TOF [M+Na]⁺ mass spectra from PA, WA and BRS aqueous fractions. Figure S7—Effect of PA on the metallic surface after 24 h immersion in neutral pH corrosive solution without PA and 1.0 g·L⁻¹ of PA. A—Metallic surface after 24 h immersion in neutral pH corrosive solution; B—Black protective film formation after 24 h immersion in neutral pH corrosive solution with 1.0 g·L⁻¹ of PA; and C—metallic surface after black film removal. Figure S8—Nyquist plot for carbon steel AISI 1020 in a neutral pH corrosive solution for purple açai (PA) crude extract in 1.0 g·L⁻¹. The control represents the absence of any inhibitor. Figure S9—Bode plot for carbon steel AISI 1020 in a neutral pH corrosive solution purple açai (PA) crude extract in 1.0 g·L⁻¹. The control represents the absence of any inhibitor. Relation between log frequency (Hz) and phase angle (°) and log impedance modules (Ω·cm⁻²).

Author Contributions: Conceptualization, G.R.M., D.G., A.J.R.d.S., D.S.A.; methodology, G.R.M., D.G., M.T.S.L., L.Y.R., E.F.C.S., A.J.R.d.S.; software, A.J.R.d.S.; formal analysis, G.R.M., D.G., U.L.M.d.P.; investigation, G.R.M., A.J.R.d.S., D.S.A.; resources, C.S.A., D.S.A.; data curation, G.R.M., D.G.; writing—original draft preparation, G.R.M., D.G.; writing—review and editing, M.d.S.P.d.O., M.T.S.L., L.Y.R., E.F.C.S., A.J.R.d.S., C.S.A., D.S.A.; visualization, M.d.S.P.d.O.; supervision, M.T.S.L., L.Y.R., E.F.C.S., A.J.R.d.S.; project administration, C.S.A., D.S.A.; funding acquisition, C.S.A., D.S.A. All authors have read and agreed to the published version of the manuscript.

Funding: This study was financed in part by the Coordination for the Improvement of Higher Education Personnel (CAPES), Finance Code 001. The Brazilian National Council for Scientific and

Technological Development (CNPq grant number 310057/2019-1) and Carlos Chagas Filho Foundation for Research Support of the State of Rio de Janeiro (FAPERJ grant number CNE 233.939/2017).

Institutional Review Board Statement: Not applicable.

Informed Consent Statement: Not applicable.

Data Availability Statement: Not applicable.

Acknowledgments: This study was financed in part by the Coordination for the Improvement of Higher Education Personnel (CAPES), Finance Code 001. The authors are also grateful to The Brazilian National Council for Scientific and Technological Development (CNPq grant number 310057/2019-1) and Carlos Chagas Filho Foundation for Research Support of the State of Rio de Janeiro (FAPERJ grant number CNE 233.939/2017) for the financial support. Centro de Espectrometria de Massas de Biomoléculas (CEMbio/UFRJ) and the Central Analítica de IPPN/UFRJ are thanked for the analysis. The authors thank José Guilherme Soares Maia, who graciously granted seeds for the conceived study, and Lucio Mendes Cabral for the HILIC–HPLC–FLD analysis.

Conflicts of Interest: The authors declare no conflict of interest.

Sample Availability: Samples of the compounds are not available from the authors.

References

1. Smith, N. *Palms and People in the Amazon*; Geobotany Studies; Springer International Publishing: Cham, Switzerland, 2015; ISBN 978-3-319-05508-4.
2. Heinrich, M.; Dhanji, T.; Casselman, I. Açai (*Euterpe oleracea* Mart.)—A phytochemical and pharmacological assessment of the species' health claims. *Phytochem. Lett.* **2011**, *4*, 10–21. [[CrossRef](#)]
3. Wycoff, W.; Luo, R.; Schauss, A.G.; Neal-Kababick, J.; Sabaa-Srur, A.U.O.; Maia, J.G.S.; Tran, K.; Richards, K.M.; Smith, R.E. Chemical and nutritional analysis of seeds from purple and white açai (*Euterpe oleracea* Mart.). *J. Food Compos. Anal.* **2015**, *41*, 181–187. [[CrossRef](#)]
4. Schauss, A.G. Advances in the study of the health benefits and mechanisms of action of the pulp and seed of the Amazonian palm fruit, *Euterpe oleracea* Mart., known as “Açai”. In *Fruits, Vegetables, and Herbs*; Elsevier Inc.: Oxford, UK, 2016; ISBN 9780128029893.
5. da Silveira, T.F.F.; de Souza, T.C.L.; Carvalho, A.V.; Ribeiro, A.B.; Kuhnle, G.G.C.; Godoy, H.T. White açai juice (*Euterpe oleracea*): Phenolic composition by LC-ESI-MS/MS, antioxidant capacity and inhibition effect on the formation of colorectal cancer related compounds. *J. Funct. Foods* **2017**, *36*, 215–223. [[CrossRef](#)]
6. Rufino, M.d.S.M.; Pérez-Jiménez, J.; Arranz, S.; Alves, R.E.; de Brito, E.S.; Oliveira, M.S.P.; Saura-Calixto, F. Açai (*Euterpe oleracea*) “BRS Pará”: A tropical fruit source of antioxidant dietary fiber and high antioxidant capacity oil. *Food Res. Int.* **2011**, *44*, 2100–2106. [[CrossRef](#)]
7. Melo, P.S.; Selani, M.M.; Gonçalves, R.H.; de Oliveira Paulino, J.; Massarioli, A.P.; de Alencar, S.M. Açai seeds: An unexplored agro-industrial residue as a potential source of lipids, fibers, and antioxidant phenolic compounds. *Ind. Crops Prod.* **2021**, *161*, 113204. [[CrossRef](#)]
8. Pessoa, J.D.C.; Arduin, M.; Martins, M.A.; de Carvalho, J.E.U. Characterization of açai (*E. oleracea*) fruits and its processing residues. *Braz. Arch. Biol. Technol.* **2010**, *53*, 1451–1460. [[CrossRef](#)]
9. Monteiro, A.F.; Miguez, I.S.; Silva, J.P.R.B.; da Silva, A.S. High concentration and yield production of mannose from açai (*Euterpe oleracea* Mart.) seeds via mannanase-catalyzed hydrolysis. *Sci. Rep.* **2019**, *9*, 10939. [[CrossRef](#)]
10. Melo, P.S.; de Oliveira Rodrigues Arrivetti, L.; de Alencar, S.M.; Skibsted, L.H. Antioxidative and prooxidative effects in food lipids and synergism with α -tocopherol of açai seed extracts and grape rachis extracts. *Food Chem.* **2016**, *213*, 440–449. [[CrossRef](#)]
11. Martins, G.R.; do Amaral, F.R.L.; Brum, F.L.; Mohana-Borges, R.; de Moura, S.S.T.; Ferreira, F.A.; Sangenito, L.S.; Santos, A.L.S.; Figueiredo, N.G.; da Silva, A.S. Chemical characterization, antioxidant and antimicrobial activities of açai seed (*Euterpe oleracea* Mart.) extracts containing A- and B-type procyanidins. *LWT* **2020**, *132*, 109830. [[CrossRef](#)]
12. Barros, L.; Calhelha, R.C.; Queiroz, M.J.R.P.; Santos-Buelga, C.; Santos, E.A.; Regis, W.C.B.; Ferreira, I.C.F.R. The powerful in vitro bioactivity of *Euterpe oleracea* Mart. seeds and related phenolic compounds. *Ind. Crops Prod.* **2015**, *76*, 318–322. [[CrossRef](#)]
13. De Moura, R.S.; Pires, K.M.P.; Ferreira, T.S.; Lopes, A.A.; Nesi, R.T.; Resende, A.C.; Sousa, P.J.C.; da Silva, A.J.R.; Porto, L.C.; Valença, S.S. Addition of açai (*Euterpe oleracea*) to cigarettes has a protective effect against emphysema in mice. *Food Chem. Toxicol.* **2011**, *49*, 855–863. [[CrossRef](#)] [[PubMed](#)]
14. De Oliveira, P.R.B.; Da Costa, C.A.; De Bem, G.F.; Cordeiro, V.S.C.; Santos, I.B.; De Carvalho, L.C.R.M.; Da Conceição, E.P.S.; Lisboa, P.C.; Ognibene, D.T.; Sousa, P.J.C.; et al. *Euterpe oleracea* Mart.-derived polyphenols protect mice from diet-induced obesity and fatty liver by regulating hepatic lipogenesis and cholesterol excretion. *PLoS ONE* **2015**, *10*, e0143721. [[CrossRef](#)]
15. Zapata-Sudo, G.; da Silva, J.S.; Pereira, S.L.; Souza, P.J.; de Moura, R.S.; Sudo, R.T. Oral treatment with *Euterpe oleracea* Mart. (açai) extract improves cardiac dysfunction and exercise intolerance in rats subjected to myocardial infarction. *BMC Complement. Altern. Med.* **2014**, *14*, 227. [[CrossRef](#)] [[PubMed](#)]

16. Hümmer, W.; Schreier, P. Analysis of proanthocyanidins. *Mol. Nutr. Food Res.* **2008**, *52*, 1381–1398. [[CrossRef](#)]
17. Ou, K.; Gu, L. Absorption and metabolism of proanthocyanidins. *J. Funct. Foods* **2014**, *7*, 43–53. [[CrossRef](#)]
18. Ping, L.; Brosse, N.; Chrusciel, L.; Navarrete, P.; Pizzi, A. Extraction of condensed tannins from grape pomace for use as wood adhesives. *Ind. Crops Prod.* **2011**, *33*, 253–257. [[CrossRef](#)]
19. Filgueira, D.; Moldes, D.; Fuentealba, C.; García, D.E. Condensed tannins from pine bark: A novel wood surface modifier assisted by laccase. *Ind. Crops Prod.* **2017**, *103*, 185–194. [[CrossRef](#)]
20. Shirmohammadi, Y.; Efhamisizi, D.; Pizzi, A. Tannins as a sustainable raw material for green chemistry: A review. *Ind. Crops Prod.* **2018**, *126*, 316–332. [[CrossRef](#)]
21. Neto, R.T.; Santos, S.A.O.; Oliveira, J.; Silvestre, A.J.D. Biorefinery of high polymerization degree proanthocyanidins in the context of circular economy. *Ind. Crops Prod.* **2020**, *151*, 112450. [[CrossRef](#)]
22. Koch, G.; Varney, J.; Thopson, N.; Moghissi, O.; Gould, M.; Payer, J. International Measures of Prevention, Application, and Economics of Corrosion Technologies Study. *NACE Int.* **2016**, 1–216.
23. Miralrio, A.; Vázquez, A.E. Plant extracts as green corrosion inhibitors for different metal surfaces and corrosive media: A review. *Processes* **2020**, *8*, 942. [[CrossRef](#)]
24. Tan, K.W.; Kassim, M.J.; Oo, C.W. Possible improvement of catechin as corrosion inhibitor in acidic medium. *Corros. Sci.* **2012**, *65*, 152–162. [[CrossRef](#)]
25. Agi, A.; Junin, R.; Rasol, M.; Gbadamosi, A.; Gunaji, R. Treated *Rhizophora mucronata* tannin as a corrosion inhibitor in chloride solution. *PLoS ONE* **2018**, *13*, e0200595. [[CrossRef](#)]
26. Tan, K.W.; Kassim, M.J. A correlation study on the phenolic profiles and corrosion inhibition properties of mangrove tannins (*Rhizophora apiculata*) as affected by extraction solvents. *Corros. Sci.* **2011**, *53*, 569–574. [[CrossRef](#)]
27. Guedes, D.; Martins, G.R.; Jaramillo, L.Y.A.; Simas Bernardes Dias, D.; da Silva, A.J.R.; Lutterbach, M.T.S.; Reznik, L.Y.; Sérvulo, E.F.C.; Alviano, C.S.; Alviano, D.S. Proanthocyanidins with Corrosion Inhibition Activity for AISI 1020 Carbon Steel under Neutral pH Conditions of Coconut (*Cocos nucifera* L.) Husk Fibers. *ACS Omega* **2021**, *6*, 6893–6901. [[CrossRef](#)]
28. Calicioglu, Ö.; Bogdanski, A. Linking the bioeconomy to the 2030 sustainable development agenda: Can SDG indicators be used to monitor progress towards a sustainable bioeconomy? *New Biotechnol.* **2021**, *61*, 40–49. [[CrossRef](#)]
29. Romão, M.H.; de Bem, G.F.; Santos, I.B.; de Andrade Soares, R.; Ognibene, D.T.; de Moura, R.S.; da Costa, C.A.; Resende, Â.C. Açai (*Euterpe oleracea* Mart.) seed extract protects against hepatic steatosis and fibrosis in high-fat diet-fed mice: Role of local renin-angiotensin system, oxidative stress and inflammation. *J. Funct. Foods* **2020**, *65*, 103726. [[CrossRef](#)]
30. de Souza da Silva, A.; Nunes, D.V.Q.; de Carvalho, L.C.d.R.M.; Santos, I.B.; de Menezes, M.P.; de Bem, G.F.; da Costa, C.A.; de Moura, R.S.; Resende, A.C.; Ognibene, D.T. Açai (*Euterpe oleracea* Mart) seed extract protects against maternal vascular dysfunction, hypertension, and fetal growth restriction in experimental preeclampsia. *Hypertens. Pregnancy* **2020**, *39*, 211–219. [[CrossRef](#)]
31. Monteiro, E.B.; Soares, E.D.R.; Trindade, P.L.; Bem, G.F.; Resende, A.C.; Passos, M.M.C.D.F.; Soulage, C.O.; Daleprane, J.B. Uraemic toxin-induced inflammation and oxidative stress in human endothelial cells: Protective effect of polyphenol-rich extract from açai. *Exp. Physiol.* **2020**, *105*, 542–551. [[CrossRef](#)] [[PubMed](#)]
32. Makkar, H.P.S. *Quantification of Tannins in Tree and Shrub Foliage*; Springer: Dordrecht, The Netherlands, 2003; ISBN 978-90-481-6428-8.
33. Kelm, M.A.; Johnson, J.C.; Robbins, R.J.; Hammerstone, J.F.; Schmitz, H.H. High-performance liquid chromatography separation and purification of cacao (*Theobroma cacao* L.) procyanidins according to degree of polymerization using a diol stationary phase. *J. Agric. Food Chem.* **2006**, *54*, 1571–1576. [[CrossRef](#)] [[PubMed](#)]
34. Robbins, R.J.; Leonczak, J.; Johnson, J.C.; Li, J.; Kwik-Uribe, C.; Prior, R.L.; Gu, L. Method performance and multi-laboratory assessment of a normal phase high pressure liquid chromatography-fluorescence detection method for the quantitation of flavanols and procyanidins in cocoa and chocolate containing samples. *J. Chromatogr. A* **2009**, *1216*, 4831–4840. [[CrossRef](#)]
35. Lin, L.-Z.; Sun, J.; Chen, P.; Monagas, M.J.; Harnly, J.M. UHPLC-PDA-ESI/HRMS n Profiling Method To Identify and Quantify Oligomeric Proanthocyanidins in Plant Products. *J. Agric. Food Chem.* **2014**, *62*, 9387–9400. [[CrossRef](#)] [[PubMed](#)]
36. Soares, E.R.; Monteiro, E.B.; de Bem, G.F.; Inada, K.O.P.; Torres, A.G.; Perrone, D.; Soulage, C.O.; Monteiro, M.C.; Resende, A.C.; Moura-Nunes, N.; et al. Up-regulation of Nrf2-antioxidant signaling by Açai (*Euterpe oleracea* Mart.) extract prevents oxidative stress in human endothelial cells. *J. Funct. Foods* **2017**, *37*, 107–115. [[CrossRef](#)]
37. Monagas, M.; Quintanilla-López, J.E.; Gómez-Cordovés, C.; Bartolomé, B.; Lebrón-Aguilar, R. MALDI-TOF MS analysis of plant proanthocyanidins. *J. Pharm. Biomed. Anal.* **2010**, *51*, 358–372. [[CrossRef](#)]
38. Pal, A.; Das, C. A novel use of solid waste extract from tea factory as corrosion inhibitor in acidic media on boiler quality steel. *Ind. Crops Prod.* **2020**, *151*, 112468. [[CrossRef](#)]
39. Sastri, V.S. *Green Corrosion Inhibitors*; John Wiley & Sons, Inc.: Hoboken, NJ, USA, 2011; ISBN 9781118015438.
40. Popov, B.N. *Corrosion Engineering*; Elsevier: Amsterdam, The Netherlands, 2015; ISBN 9780444627223.
41. Zmozinski, A.V.; Peres, R.S.; Freiberger, K.; Ferreira, C.A.; Tamborim, S.M.M.; Azambuja, D.S. Zinc tannate and magnesium tannate as anticorrosion pigments in epoxy paint formulations. *Prog. Org. Coat.* **2018**, *121*, 23–29. [[CrossRef](#)]
42. Merchan-Arenas, D.; Sanabria-Cala, J.; Cortes-Castillo, L.; Camacho, D.; Vesga, G.; Peña-Ballesteros, D.; Kouznetsov, V. Electrochemical evaluation of the corrosion rate inhibition capacity of eugenol, o-eugenol and diphenol, on AISI 1020 Steel Exposed to 1M HCl Medium. *Chem. Eng. Trans.* **2018**, *64*, 247–252. [[CrossRef](#)]

43. Saxena, A.; Prasad, D.; Haldhar, R.; Singh, G.; Kumar, A. Use of *Saraca ashoka* extract as green corrosion inhibitor for mild steel in 0.5 M H₂SO₄. *J. Mol. Liq.* **2018**, *258*, 89–97. [[CrossRef](#)]
44. Nardeli, J.V.; Fugivara, C.S.; Taryba, M.; Pinto, E.R.P.; Montemor, M.F.; Benedetti, A.V. Tannin: A natural corrosion inhibitor for aluminum alloys. *Prog. Org. Coat.* **2019**, *135*, 368–381. [[CrossRef](#)]
45. Kennedy, J.A. Proanthocyanidins: Extraction, Purification, and Determination of Subunit Composition by HPLC. *Curr. Protoc. Food Anal. Chem.* **2002**, *6*, I1.4.1–I1.4.11. [[CrossRef](#)]
46. Karonen, M.; Liimatainen, J.; Sinkkonen, J. Birch inner bark procyanidins can be resolved with enhanced sensitivity by hydrophilic interaction HPLC-MS. *J. Sep. Sci.* **2011**, *34*, 3158–3165. [[CrossRef](#)] [[PubMed](#)]